Surgical and Radiologic Anatomy (2022) 44:391–397
https://doi.org/10.1007/s00276-021-02876-6

ORIGINAL ARTICLE

"Hammock" suspending the superior ophthalmic vein: a magnetic resonance imaging study

Satoshi Tsutsumi[1] · **Hideo Ono**[2] · **Hisato Ishii**[1]

Received: 18 November 2021 / Accepted: 22 December 2021 / Published online: 3 January 2022

Abstract

Purpose The present study aimed to explore the hammock-like structure suspending the superior ophthalmic vein (SOV) using magnetic resonance imaging (MRI).

Methods Following conventional MRI examination, 93 outpatients underwent thin-sliced, coronal T2-weighted and contrast imaging of the orbit.

Results SOVs were consistently detected in all 93 patients. In 90.3% of patients, a hammock-like structure suspending the SOV was identified, which was present on both sides in 64.5% of patients. The structure was frequently located in the anterior and middle thirds of the retrobulbar orbit, suspended from the superolateral corner of the orbital walls. The medial edge of the hammocks did not reach the orbital walls; therefore, they partially encased the SOV. The morphology of the hammock was highly variable between patients, although none were tethered to the extraocular muscles. In addition, a septal band connecting the hammock and optic sheath was identified in 36.6% of patients, most frequently located in the posterior third of the retrobulbar orbit.

Conclusions The hammock suspending the SOV and the septal band connecting the hammock and optic sheath may be structures that loosely anchor the SOV to the orbital fat to maintain a constant SOV flow, in addition to preventing excessive bends and obstructions.

Keywords Hammock · Magnetic resonance imaging · Optic sheath · Superior ophthalmic vein

Introduction

The superior ophthalmic vein (SOV) is the largest vein of the orbit, functioning as an emissary vein by connecting between the intracranial and extracranial venous systems. It commonly arises in the superomedial orbit, traveling posterior in the mediolateral direction below the superior rectus muscle, crossing over the optic sheath, then passing through the lateral sector of the superior orbital fissure, and finally connecting to the superolateral part of the cavernous sinus (Fig. 1). In the subcutaneous tissue communicating with the superomedial orbit, the most anterior segment of the SOV connects with the facial and supraorbital veins [10, 13, 15]. As SOVs can be affected by a variety of pathologies, including venous thrombosis, carotid cavernous fistula, spontaneous intracranial hypotension, Graves orbitopathy, orbital tumor and pseudotumor, and parasellar meningioma, it has been studied extensively to determine the normal anatomy and flow patterns under physiological conditions [1, 2, 5, 7–17]. A septal structure located in the middle and posterior parts of the orbit that suspends the SOV has been documented as a "hammock" of the SOV in a limited number of subjects [3, 4, 6, 13]. Such "hammock" was sporadically documented as fibrous band or septal structure in studies with cadaver dissection and magnetic resonance imaging (MRI). To the best of our knowledge, no study has yet described such hammocks in detail and the knowledge of them is still fragmentary. Therefore, the present study aimed to explore the structures using MRI.

✉ Satoshi Tsutsumi
shotaro@juntendo-urayasu.jp

[1] Department of Neurological Surgery, Juntendo University Urayasu Hospital, 2-1-1 Tomioka, Urayasu, Chiba 279-0021, Japan

[2] Division of Radiological Technology, Medical Satellite Yaesu Clinic, Tokyo, Japan

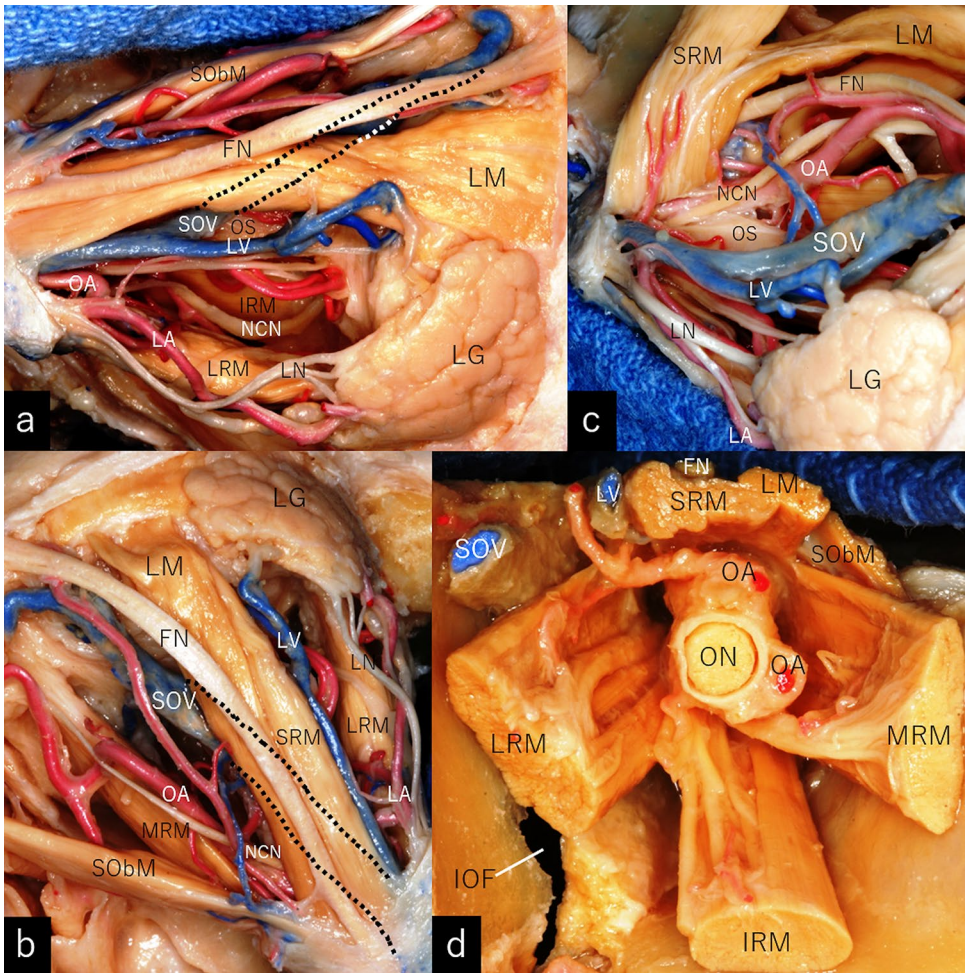

Fig. 1 Superolateral (**a**), posteromedial (**b**), and anterolateral (**c**) views, and frontal view at the orbital apex (**d**) of an example dissected right orbit showing the location of the superior ophthalmic vein in the orbit and its characteristic course in a lateromedial direction below the superior rectus muscle, crossing over the optic sheath. In (**c**), the superior rectus and levator muscles are reflected superiorly. *FN* frontal nerve; *IOF* inferior orbital fissure; *IRM* inferior rectus muscle; *LA* lacrimal artery; *LG* lacrimal gland; *LM* levator muscle; *LN* lacrimal nerve; *LRM* lateral rectus muscle; *LV* lacrimal vein; *MRM* medial rectus muscle; *NCN* nasociliary nerve; *OA* ophthalmic artery; *ON* optic nerve; *OS* optic sheath; *SOV* superior ophthalmic vein; *SObM* superior oblique muscle; *SRM* superior rectus muscle; dotted lines: course of the superior ophthalmic vein below the superior rectus muscle

Materials and methods

This retrospective study enrolled 93 outpatients who presented to our hospital between September 2011 and August 2013 with headache, dizziness, vertigo, tinnitus, hemisensory disturbance, scintillating scotoma, and focal seizures, and underwent cerebral MRI covering the entire orbits. The patient population included 48 men and 45 women with ages ranging from 12 to 81 years (mean, 53.3 ± 16.0 years). None of the patients had a history of cerebral or orbital vascular diseases, SOV thrombosis, intracranial or orbital tumors, Graves orbitopathy, spontaneous intracranial hypotension, or hydrocephalus. These pathologies were excluded by detailed interviews at the presentation and following initial, conventional MRI examinations using axial T1-weighted, T2-weighted, T2-gradient echo, fluid-attenuated inversion recovery, and diffusion-weighted sequences. Thereafter, the patients underwent thin-sliced, coronal T2-weighted imaging covering the entire course of the intraorbital optic nerve. The following parameters were used for each sequence: repetition time, 3,500.0 ms; echo time, 90.0 ms; slice thickness, 2.0 mm; interslice gap, 0 mm; matrix, 300 × 189; field of view, 200 mm × 200 mm; flip angle, 90°; and scan duration, 2 min 40 s. Furthermore, these patients underwent contrast examination with intravenous gadolinium infusion (0.1 mmol/kg) in the axial, coronal, and sagittal planes involving the whole cranial vault. The following parameters were consistently adopted: repetition time, 4.1 ms; echo time, 1.92 ms; slice thickness, 1 mm; interslice gap, 0 mm; matrix, 320 × 320; field of view, 250 mm; flip angle, 13°; and scan duration, 7 min 25 s. In this study, only coronal images were used for comparison with the coronal T2-weighted images. All examinations were performed using a 3.0-T MRI scanner (Achieva R2.6; Philips Medical Systems, Best, The Netherlands). The obtained imaging data were transferred to a workstation (Virtual Place Lexus64, 64 edition, AZE, Tokyo, Japan) and analyzed independently by two of the authors (S.T. and H.I.). Initially, based on comparison with the post-contrast coronal images, the orbital SOV segments were identified on the coronal T2-weighted images sectioned at the same level on the post-contrast

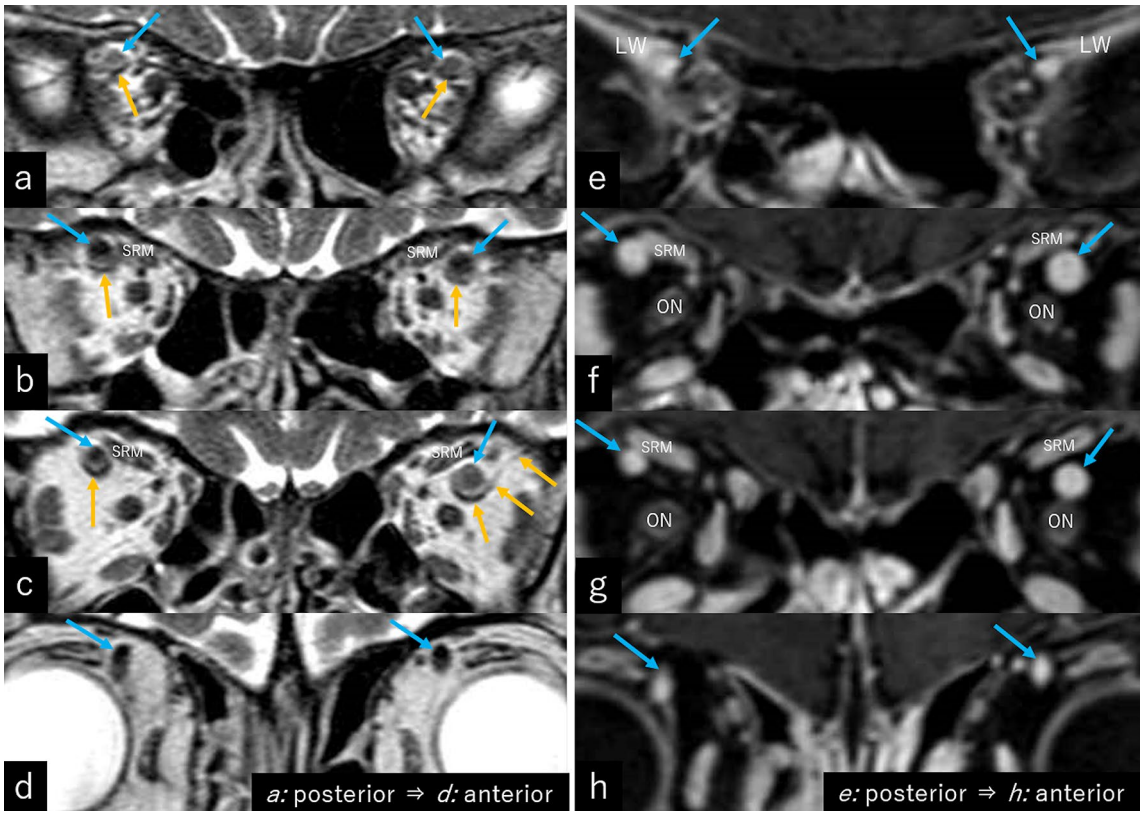

Fig. 2 Coronal T2- (**a–d**) and post-contrast T1-weighted (**e–f**) magnetic resonance images of a patient performed at the same levels of the orbit, posterior (**a**, **e**), middle (**b**, **f**), and anterior (**c, g**) thirds of the retrobulbar orbits and at the equator of eyeballs (**d**, **h**), showing the hammock suspending the superior ophthalmic vein that is determined based on the referral post-contrast images (**a–c**, orange arrows). *LW* lesser wing of the sphenoid; *ON* optic nerve; *SRM* superior rectus muscle; blue arrow: superior ophthalmic vein

images. Then, a hammock-like structure suspending the SOV was searched on the coronal T2-weighted images (Fig. 2). Such structure was consistently expressed as "hammock" in this study. Next, on serial coronal T2-weighted images, the hammock suspension of the SOV was assessed along with other septal structures associated with the hammock (Fig. 3). For convenience, the retrobulbar orbital cavity was divided into three parts: the anterior, middle, and posterior thirds with the posterior limit of the globe and that of the orbital apex as the landmarks. In each orbital section, the identified hammock and septal bands were recorded. A segment of the SOV coursing anterior to the posterior limit of the globe and associated hammock-like structures were not included in the analysis.

The present study was approved by an ethical review board and conducted in accordance with the guidelines of our institution for human research. Written informed consent both for the examination and retrospective use of images were obtained from all participants.

Results

On serial coronal images, SOVs were identified in all 93 patients on both sides. A hammock supporting the SOV was identified in 84 patients (90.3%), 13 (14.0%) on the right, 11 (11.8%) on the left, and 60 (64.5%) on both sides. There were no common demographical points or morphology of the orbit in patients without identified hammock. In the bilateral cases, the locations of hammock were commonly asymmetric between the two orbits. Such hammock was located in the anterior third of the orbit in 64 patients, and was found in the middle and posterior third in 63 and 47 patients, respectively (Table 1). The hammock was delineated as a linear hypointense, U-shaped structure in the retrobulbar region with the lateral edge suspended from the superolateral corner of the orbital wall. None of the medial edge of the identified hammocks reached the orbital walls, partially encasing the transmitting SOV (Fig. 4). The morphology of the identified hammocks

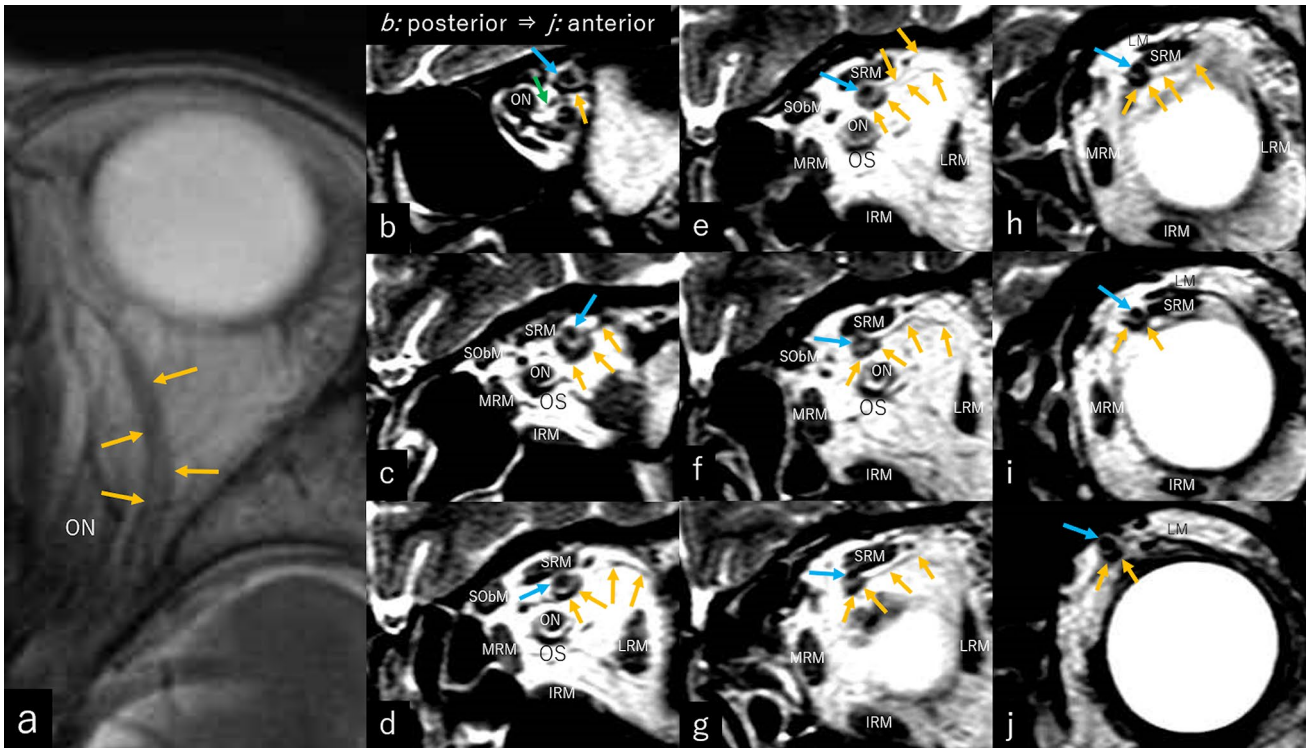

Fig. 3 Axial image at the level of the superior ophthalmic vein (**a**) and serial coronal images (**b–j**) on T2-weighted magnetic resonance imaging of the same patient showing the hammock suspending the superior ophthalmic vein suspended from the superolateral corner of the left orbit (**a–j**, orange arrows) and a septal band connecting the hammock and optic sheath (**b**, green arrow). *IRM* inferior rectus muscle; *LM* levator muscle; *LRM* lateral rectus muscle; *MRM* medial rectus muscle; *ON* optic nerve; *OS* optic sheath; *SObM* superior oblique muscle; *SRM* superior rectus muscle; blue arrow: superior ophthalmic vein

Table 1 Summary of the identification ratios of the hammock

Side		Location	
Right	13/93 (14.0%)	Anterior third	64/93 (68.8%)
Left	11/93 (11.8%)	Middle third	63/93 (67.7%)
Right and left	60/93 (64.5%)	Posterior third	47/93 (50.5%)
Total	84/93 (90.3%)		

showed high interindividual variability, while none of them were tethered to the extraocular muscles, lying in the orbital fat (Fig. 5). Length of the hammock was longer in the more anterior of the orbit. In addition, a septal band connecting the hammock and optic sheath was identified in 34 of 93 patients (36.6%), 16 (17.2%) on the right, 11 (11.8%) on the left, and 7 (7.5%) on both sides. The band was located in the anterior third of the orbit in 5 patients (5.4%), while it was found in the middle and posterior third in 11 (11.8%) and 21 (22.6%) patients, respectively (Table 2). In 3 of 37 patients, the band was found both in the anterior and middle thirds. Morphological variability was also observed with varying lengths that were not correlated to the location in the orbit (Fig. 6). Also, the location of the band was not correlated to that of the hammock. The characteristics of the hammock and septal band were consistent in patients with them in two orbits.

Discussion

The connective tissue system of the orbit has received less attention, probably as it is currently unknown which optimal methodologies are required to elucidate it. In the present study, using thin-sliced, coronal MRI, hammocks that suspend the SOV from the superolateral corner of the retrobulbar orbits were delineated in more than 90% of cases, and bilaterally in 64.5% of cases. In addition, septal bands connecting the hammock and optic sheath were identified in 36.6% of cases, frequently in the posterior and middle thirds of the retrobulbar orbit. Such hammocks were more frequently identified in the anterior and middle thirds of the retrobulbar orbit, while they were less frequent in the posterior third. Previous studies identified the hammocks only in the orbital apex [3, 6, 13]. This may mainly derive from the characteristics of T2-weighted imaging that can favorably discriminate such septal structure when surrounded by a plenty amount of orbital fat, while it is difficult to discriminate in the narrow orbital apex with scant fat. The hammocks

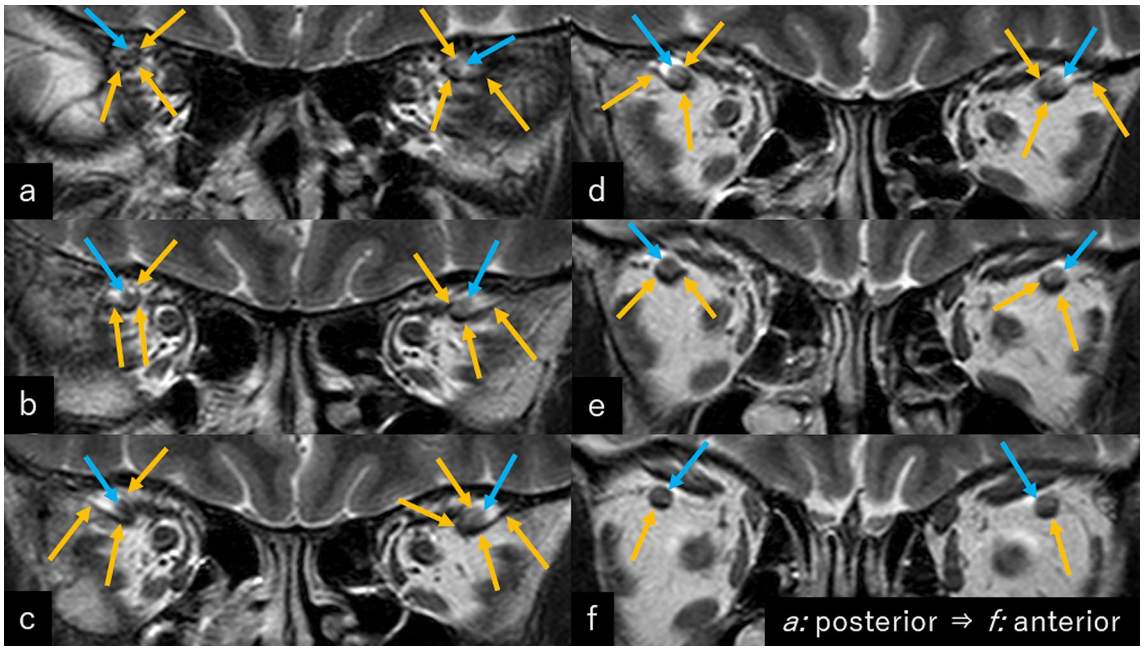

Fig. 4 Serial images of the coronal T2-weighted magnetic resonance imaging of a patient at the level of the posterior (**a**, **b**), middle (**c**, **d**), and anterior (**e**, **f**) thirds of the retrobulbar orbit showing the hypointense, U-shaped hammock suspending the superior ophthalmic veins with the lateral edges suspended from the superolateral corner of the retrobulbar orbits (**a–d**, orange arrows). Note that the medial edge of the hammock does not reach the orbital wall, partially encasing the suspended superior ophthalmic vein. Blue arrow: superior ophthalmic vein

may exist throughout the orbit, not localized in the orbital apex, in association with the SOV. In the orbital apex, these hammocks may not be identified on MRI even if they are actually present. Furthermore, given that the hammock and SOV are anchored in the orbital fat and not tethered to the extraocular muscles, the hammock may facilitate to maintain the morphology and flow of the SOV at extraocular movements or compression by tumorous lesions. Also, in this study, the septal band was more frequently identified in the posterior third of the retrobulbar orbit, different from the hammocks, compared to the middle and anterior thirds. This may derive from an easy identification of the band for surrounded by the orbital fat, not adjacent to the orbital muscular or vascular structures, in addition to the possible predisposition to the orbital apex. Only a few studies have been conducted on the connective tissue systems of the orbits [3, 4, 6]. Investigation of the tissue can provide novel insights into the anatomofunctional implications of SOVs and relevant structures.

The present study had several limitations. Our study was performed retrospectively. The group of subjects was not a population with homogenous age and sex distribution. In addition, the hammocks of the SOVs and septal bands were assessed only on coronal T2-weighted images. Therefore, the outcomes obtained should be validated by further investigations using an appropriate methodology such as observations on thin-sliced, serial sections. Despite these limitations, we believe that the findings of this study can help to understand the SOV and the orbital connective tissue system suspending it.

Conclusions

The hammock suspending the SOV and septal band connecting the hammock and optic sheath may be structures that loosely anchor the SOV to the orbital fat to maintain a constant SOV flow, in addition to preventing excessive bending and obstruction.

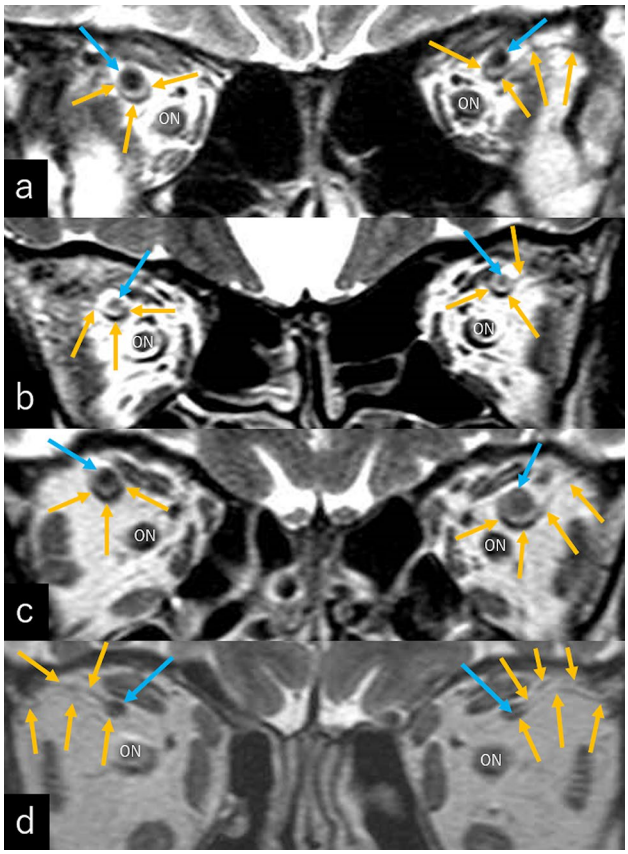

Fig. 5 Coronal T2-weighted magnetic resonance images of different patients at the level of the posterior (**a**, **b**), middle (**c**), and anterior (**d**) thirds of the retrobulbar orbits showing the hammocks suspending the superior ophthalmic veins with variable morphologies (**a–d**, orange arrows). *ON* optic nerve; blue arrow: superior ophthalmic vein

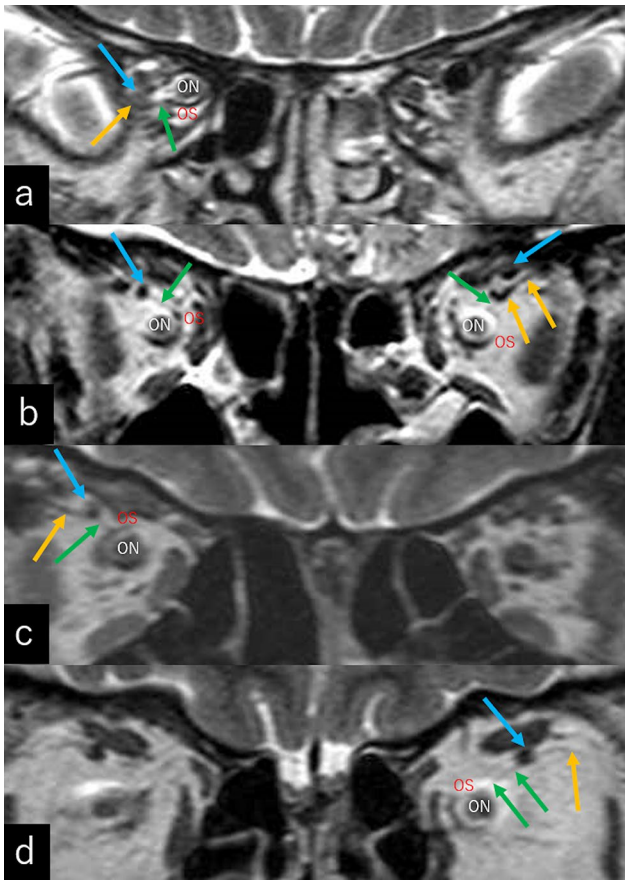

Fig. 6 Coronal T2-weighted magnetic resonance images of different patients at the level of the posterior (**a**), middle (**b**), and anterior (**c**, **d**) thirds of the retrobulbar orbits showing the septal band with varying lengths that connects between the hammock suspending the superior ophthalmic vein and the optic sheath [**a–d**, green arrow(s)]. *ON:* optic nerve; *OS:* optic sheath; blue arrow: superior ophthalmic vein; orange arrow(s): hammock suspending the superior ophthalmic vein

Table 2 Summary of the identification ratios of the septal band

Side		Location	
Right	16/93 (17.2%)	Anterior third	5/93 (5.4%)
Left	11/93 (11.8%)	Middle third	11/93 (11.8%)
Right and left	7/93 (7.5%)	Posterior third	21/93 (22.6%)
Total	34/93 (36.6%)		

Author contributions All the authors have equally contributed to the study.

Funding No funding was received for this study.

Declarations

Conflict of interest The authors have no conflicts of interest to declare regarding the materials or methods used, or the findings presented in this study.

Ethical approval All procedures performed in the study were in accordance with the ethical standards of the institutional and/or national research committee in addition to the 1964 Declaration of Helsinki and its later amendments or comparable ethical standards.

Informed consent Informed consent was obtained from all participants included in the study.

References

1. Adam CR, Shields CL, Gutman J, Kim HJ, Hayek B, Shore JW, Braunstein A, Levin F, Winn BJ, Vrcek I, Mancini R, Linden C, Choe C, Gonzalez M, Altschul D, Ortega-Gutierrez S, Paramasivam S, Fifi JT, Berenstein A, Durairaj V, Shinder R (2018) Dilated superior ophthalmic vein: clinical and radiographic features of 113 cases. Ophthalmic Plast Reconstr Surg 34:68–73
2. Bacon KT, Duchesneau PM, Weinstein MA (1977) Demonstration of the superior ophthalmic vein by high resolution computed tomography. Radiology 124:129–131

3. Bergen MP (1981) A literature review of the vascular system in the human orbit. Acta Morphol Neerl Scand 19:273–305
4. Bergen MP (1982) Some histological aspects of the structure of the connective tissue system and its relationships with the blood vessels in the human orbit. Acta Morphol Neerl Scand 20:293–308
5. Chen WT, Fuh JL, Lirng JF, Lu SR, Wu ZA, Wang SJ (2003) Collapsed superior ophthalmic veins in patients with spontaneous intracranial hypotension. Neurology 61:1265–1267
6. Ettl A, Koornneef L, Daxer A, Kramer J (1998) High-resolution magnetic resonance imaging of the orbital connective tissue system. Ophthalmic Plast Reconstr Surg 14:323–327
7. Lim LH, Scawn RL, Whipple KM, Oh SR, Lucarelli MJ, Korn BS, Kikkawa DO (2014) Spontaneous superior ophthalmic vein thrombosis: a rare entity with potentially devastating consequences. Eye (Lond) 28:348–351
8. Lirng JF, Fuh JL, Wu ZA, Lu SR, Wang SJ (2003) Diameter of the superior ophthalmic vein in relation to intracranial pressure. Am J Neuroradiol 24:700–703
9. Monteiro MLR, Angotti-Neto H, Benabou JE, Betinjane AJ (2008) Color Doppler imaging of the superior ophthalmic vein in different clinical forms of Graves' orbitopathy. Jpn J Ophthalmol 52:483–488
10. Natori Y, Rhoton AL Jr (1995) Microsurgical anatomy of the superior orbital fissure. Neurosurgery 36:762–775
11. Peyster RG, Savino PJ, Hoover ED, Schatz NJ (1984) Differential diagnosis of the enlarged superior ophthalmic vein. J Comput Assist Tomogr 8:103–107
12. Promelle V, Bouzerar R, Milazzo S, Balédent O (2018) Quantification of blood flow in the superior ophthalmic vein using phase contrast magnetic resonance imaging. Exp Eye Res 176:40–45
13. Rhoton AL Jr (2002) The orbit. Neurosurgery 51:S303–S334
14. Servo A (1982) Visualization of the superior ophthalmic vein on carotid angiography. Neuroradiology 23:141–146
15. Tsutsumi S, Nakamura M, Tabuchi T, Yasumoto Y (2015) The superior ophthalmic vein: delineation with high-resolution magnetic resonance imaging. Surg Radiol Anat 37:75–80
16. Wolfe SQ, Cumberbatch NM, Aziz-Sultan MA, Tummala R, Morcos JJ (2010) Operative approach via the superior ophthalmic vein for the endovascular treatment of carotid cavernous fistulas that fail traditional endovascular access. Neurosurgery 66:293–299
17. Zhang J, Stringer MD (2010) Ophthalmic and facial veins are not valveless. Clin Exp Ophthalmol 38:502–510